

Renewable CO₂ recycling and synthetic fuel production in a marine environment

Bruce D. Patterson^{a,b}, Frode Mo^c, Andreas Borgschulte^{a,1}, Magne Hillestad^d, Fortunat Joos^{e,f}, Trygve Kristiansen^g, Svein Sunde^h, and Jeroen A. van Bokhoven^{i,j}

^aLaboratory for Advanced Analytical Technologies, Swiss Federal Laboratories for Materials Science and Technology, CH-8600 Dübendorf, Switzerland; ^bDepartment of Physics, University of Zürich, CH-8057 Zürich, Switzerland; ^cDepartment of Physics, Norwegian University of Science and Technology, NO-7491 Trondheim, Norway; ^dDepartment of Chemical Engineering, Norwegian University of Science and Technology, NO-7491 Trondheim, Norway; ^eClimate and Environmental Physics, Physics Institute, University of Bern, CH-3012 Bern, Switzerland; ^fOeschger Center for Climate Change Research, University of Bern, CH-3012 Bern, Switzerland; ^gDepartment of Marine Technology, Norwegian University of Science and Technology, NO-7491 Trondheim, Norway; ^hDepartment of Materials Science and Engineering, Norwegian University of Science and Technology, NO-7491 Trondheim, Norway; ⁱDepartment of Chemistry and Bioengineering, ETH Zurich, CH-8093 Zurich, Switzerland; and ^jLaboratory for Catalysis and Sustainable Chemistry, Paul Scherrer Institut, CH-5232 Villigen, Switzerland

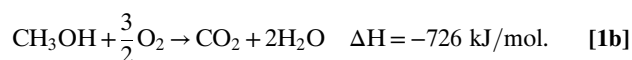
Edited by Alexis T. Bell, University of California, Berkeley, CA, and approved May 3, 2019 (received for review February 22, 2019)

A massive reduction in CO₂ emissions from fossil fuel burning is required to limit the extent of global warming. However, carbon-based liquid fuels will in the foreseeable future continue to be important energy storage media. We propose a combination of largely existing technologies to use solar energy to recycle atmospheric CO₂ into a liquid fuel. Our concept is clusters of marine-based floating islands, on which photovoltaic cells convert sunlight into electrical energy to produce H₂ and to extract CO₂ from seawater, where it is in equilibrium with the atmosphere. These gases are then reacted to form the energy carrier methanol, which is conveniently shipped to the end consumer. The present work initiates the development of this concept and highlights relevant questions in physics, chemistry, and mechanics.

renewable energy | carbon dioxide recycling | synthetic fuel | maritime structures

Limiting anthropogenic global warming to below 2 °C, a goal of the Paris Agreement of the United Nations Framework Convention on Climate Change (1), now ratified by 174 countries, will require within the coming decades the phasing out of carbon dioxide emissions from fossil fuel burning. However, in the foreseeable future, carbon-based liquid fuels will continue to play an important role, in particular for aeronautical, marine, and long-haul automotive mobility. It is therefore essential to investigate possibilities of using renewable energy to recycle CO₂ between the atmosphere and synthetic liquid fuel (2). Efforts to photochemically produce synthetic fuel from CO₂ and water (i.e., via artificial photosynthesis) show some promise (3). We propose an approach using more conventional methods, but with important unique aspects.

Methanol, CH₃OH or MeOH, is the simplest carbon-based fuel, which is liquid at ambient conditions (4). With approximately half the energy density of gasoline (15.6 MJ/L vs. 32.4 MJ/L), it can be used to power existing gas turbines, modified diesel engines, and direct methanol fuel cells. Methanol can serve as a feedstock for most petrochemical products, and by simple dehydration it can be converted to dimethyl ether, an attractive substitute for natural gas, and other hydrocarbon fuels. Methanol can be produced (5) by the catalytic hydrogenation of CO₂ [presently the largest methanol production facility using this technique is located in Iceland (6)], and MeOH burns in air to release CO₂ and water:



An attractive scenario for the production of synthetic methanol fuel is the recycling of atmospheric CO₂, the electrolytic produc-

tion of H₂, and their catalytic reaction to CH₃OH, with all of these processes powered by renewable energy. As a concept for realizing this scenario, the present work proposes the production of H₂ and the extraction of CO₂ from seawater and their catalytic reaction to produce MeOH on clusters of artificial, marine-based photovoltaic (PV)-powered “solar methanol islands” (7) (Fig. 1). We present an initial implementation plan; in view of many uncertainties, much additional work remains to be done.

Seawater as a Source of H₂ and CO₂

Renewable synthetic fuel production on distributed facilities in a marine environment has attractive features, including abundance of insolation and raw materials, avoidance of local CO₂ depletion, convenient ship-based transport to and from the sites, flexible placement close to population centers, and possible combination with aquaculture and other marine activities. The production of 1 mol of CH₃OH ideally requires 3 mol of H₂ and 1 mol of CO₂, the production/extraction of which from seawater presents serious electrochemical challenges.

Electrolysis of Seawater

The enthalpy change in splitting liquid water into gaseous hydrogen and oxygen is 286 kJ/mol H₂; industrial electrolysis plants typically require 380 kJ/mol H₂ (11) and a value of 302 kJ/mol H₂

Significance

Humankind must cease CO₂ emissions from fossil fuel burning if dangerous climate change is to be avoided. However, liquid carbon-based energy carriers are often without practical alternatives for vital mobility applications. The recycling of atmospheric CO₂ into synthetic fuels, using renewable energy, offers an energy concept with no net CO₂ emission. We propose to implement, on a large scale, marine-based artificial islands, on which solar or wind energy powers the production of hydrogen and the extraction of CO₂ from seawater and where these gases are catalytically reacted to yield liquid methanol fuel. The present work proposes specifications for such facilities and highlights essential challenges in physics, chemistry, and engineering which must be met to realize this ambitious proposal.

Author contributions: B.D.P. and J.A.v.B. proposed the concept; B.D.P., F.M., A.B., M.H., F.J., and J.A.v.B. designed the research; B.D.P., F.M., M.H., F.J., T.K., and S.S. performed the research; B.D.P. wrote the paper; and A.B., M.H., F.J., and S.S. contributed to the writing of the paper.

The authors declare no conflict of interest.

This article is a PNAS Direct Submission.

Published under the PNAS license.

¹To whom correspondence may be addressed. Email: andreas.borgschulte@empa.ch.

This article contains supporting information online at www.pnas.org/lookup/suppl/doi:10.1073/pnas.1902335116/-DCSupplemental.

Published online June 3, 2019.

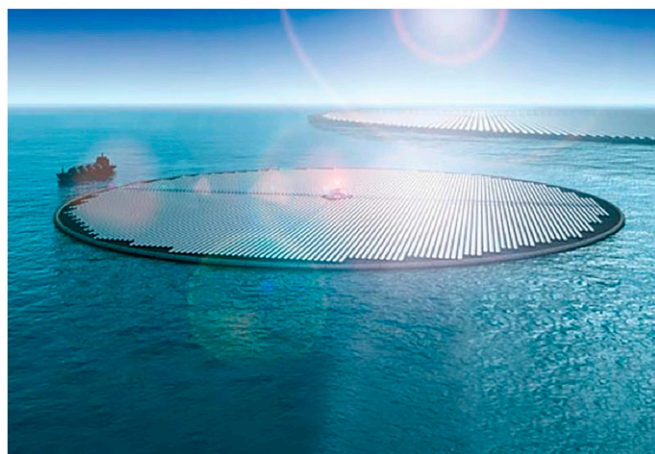
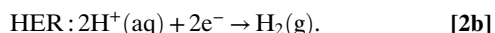
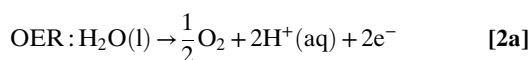


Fig. 1. Artist's conception of solar islands in the open ocean (8–10). We envisage distributed solar methanol facilities based on clusters of such islands, including electrochemical cells for H_2 production and CO_2 extraction from seawater and catalytic reactors for the production of synthetic methanol fuel. The chemical processing equipment could be installed on a fixed-hull ship. Image courtesy of Novaton.

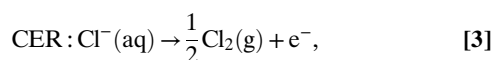
at 10 kA/m^2 has been demonstrated in the laboratory (12). The efficiency of a water electrolysis cell is determined (13) by the cell potential. This quantity is equal to the sum of ΔE_n , the reversible cell voltage (*SI Appendix*), and various “overvoltages,” which include contributions from reaction kinetics at the catalytic electrodes and from charge- and mass-transfer effects near the electrode surfaces, and an ohmic overvoltage due to the cell resistance.

For the electrolysis of pure water, the half-cell reactions (oxygen evolution reaction, OER, at the anode and hydrogen evolution reaction, HER, at the cathode) are, for acidic conditions,



As discussed in *SI Appendix*, thermodynamics dictates that the reversible potential for electrolysis at standard conditions and 25°C is $\Delta E^0 = 1.23 \text{ V}$.

In seawater electrolysis (14), undesirable competition to the OER at the anode arises from the chlorine evolution reaction, CER, which produces highly corrosive chlorine gas:



from which other chlorine-containing species, such as hypochlorite, may form (14). At standard conditions and 25°C , the reversible potential for chlorine production is 1.36 V . Since this is greater than the 1.23 V for oxygen production, one would assume that CER can be avoided by a judicious choice of operating voltage. However, theoretical work indicates that exceeding the so-called thermodynamic overpotential, related to the interdependence between the binding energies of the reaction intermediates at the catalyst surface, is required for the OER to proceed (15–17). This effectively increases the minimum potential for OER from 1.23 to $\sim 1.5 \text{ V}$, and hence favors CER over OER for seawater electrolysis.

A simple, inexpensive solution to the problem of chlorine generation at the anode is to desalinate the seawater before electrolysis: The theoretical energy expense for the desalination

of seawater, with 3.5 weight percentage NaCl, by reverse osmosis, dictated by the free-energy of mixing, is 0.987 kWh/m^3 at a recovery of 50% (18). Large-scale industrial plants, such as the $330,000\text{-m}^3/\text{d}$ installation (19) near Haifa, Israel, consume 2.2 kWh/m^3 for reverse osmosis, plus 1.5 kWh/m^3 for pre- and posttreatment (20). For our application, close access to the open ocean will reduce pumping costs and simplify brine disposal. Assuming 100% splitting of the desalinated water, the 3.7 kWh/m^3 total corresponds to 0.240 kJ/mol H_2 , or 0.063% of the energy required for (freshwater) electrolysis.

A further problem encountered in the electrolysis of seawater involves the cathode: Under the alkaline conditions that generally occur at this electrode ($\text{pH} > 11$), deposits form of insoluble $\text{Mg}(\text{OH})_2$ and CaCO_3 scale. As these deposits grow in thickness, the cell resistance increases, degrading the electrolytic efficiency. Although reverse osmosis desalination significantly reduces the concentration of Mg^{2+} and Ca^{2+} ions, the production of high-purity “process” water generally necessitates an additional deionization step using an ion exchange resin, which requires periodic regeneration (21). Alternative methods of suppressing the scale deposition include agitation, electrochemical precipitation (22), and reduction of the local pH at the cathode by feeding back a portion of the more acidic solution from the anode (23).

CO_2 Extraction from Seawater

The present fractional concentration of CO_2 in the atmosphere is $\sim 400 \text{ ppm}$, corresponding to a mass density of $0.00079 \text{ kg CO}_2/\text{m}^3$. Thus, direct capture of CO_2 from the atmosphere, for example by regenerable adsorption on organic amines, necessitates the processing of large volumes of air (24, 25). Due to the reversible, pH-dependent interconversion of carbon dioxide in water between dissolved CO_2 [carbonic acid $\text{CO}_2(\text{aq})$], bicarbonate (HCO_3^-), and carbonate (CO_3^{2-}) (26) (Fig. 24 and *SI Appendix*), the effective CO_2 concentration in seawater at a pH of 8.1, in equilibrium with the atmosphere, is $0.099 \text{ kg CO}_2/\text{m}^3$ (i.e., a factor 125 larger than in air). The time constant for the establishment of CO_2 equilibrium between the atmosphere and surface ocean waters is less than a few years (27, 28).

To extract CO_2 from seawater into a gaseous environment, it is necessary that the partial pressure of CO_2 in the water exceed that in the gas. Since the dissolution of CO_2 in water is exothermic, extraction can be performed by increasing the water temperature. However, this is an expensive option: Heating from 25 to 70°C a sufficient amount of water (2.5 m^3) to release, with 18% efficiency (29), 1 mol of CO_2 requires 470 MJ of thermal energy.

The pH-dependent chemistry of dissolved CO_2 (Fig. 24) suggests that extraction may be accomplished by making the seawater more acidic. Eisaman et al. (30) have described an electrochemical CO_2 extraction cell, which is based on bipolar membrane electrodialysis (ED) (Fig. 2B). The seawater flows through parallel channels, which are separated by alternating bipolar and anion exchange membranes. An applied electrical potential drives OH^- and Cl^- anions toward the anode and moves H^+ cations from the “base” channels to accumulate in the “acid” channels. By thus reducing the acid channel pH to below 5, CO_2 comes out of solution and is collected using membrane contactors. In such a contactor (31), the acidified seawater flows along an array of hollow fibers, with walls made of hydrophobic microporous polypropylene membrane; the CO_2 gas diffuses into the fibers and is collected by a vacuum pump. Finally, the acid and base water flows from the ED cell are recombined to yield a neutral effluent. A prototype cell extracted 59% of the dissolved CO_2 and carbonate species with an (electrical) energy expenditure of 242 kJ/mol CO_2 . Further developments and economic considerations of this device are discussed in ref. 32.

A group at the US Naval Research Laboratory is developing a device, also based on ion-exchange membranes, which extracts

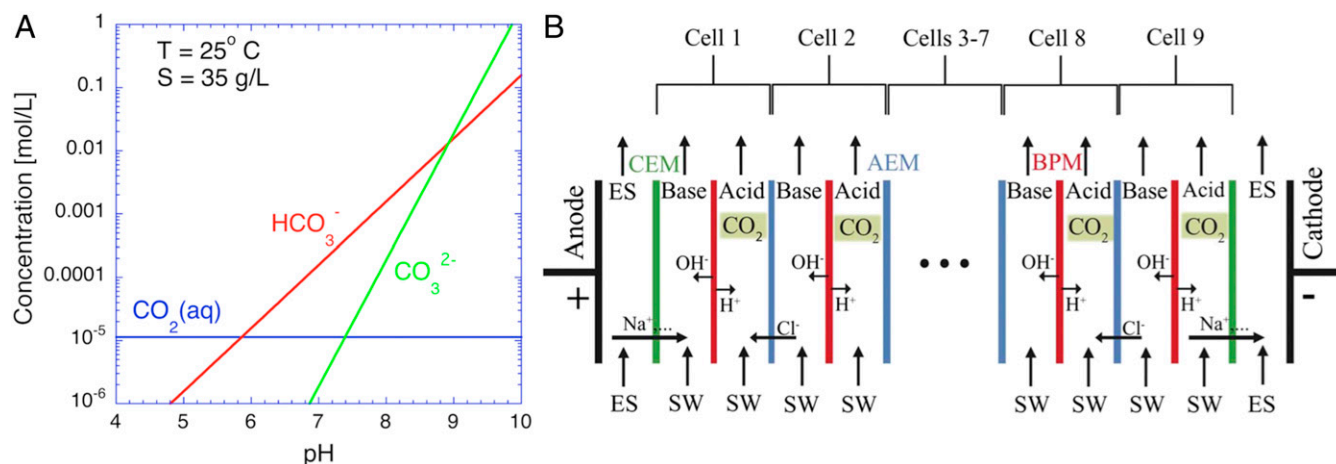
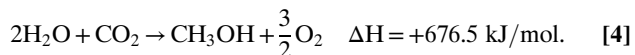


Fig. 2. The carbonate chemistry of CO₂ in seawater. (A) Effective CO₂ molar density in seawater in equilibrium with the atmosphere, due to the pH-dependent interconversion in water between gaseous CO₂, carbonic acid [CO₂(aq)], bicarbonate (HCO₃⁻), and carbonate (CO₃²⁻) (26). At the seawater pH of 8.1, the major fraction of CO₂ is bound in bicarbonate ions, which, with lowering pH, transform rapidly back to carbonic acid/gaseous CO₂. (B) The bipolar membrane ED cell of ref. 30 uses an electric current and ion-selective membranes to produce basified and acidified streams of seawater, allowing gaseous CO₂ extraction from the latter. The abbreviations are as follows: SW, seawater; ES, electrolyte solution; BPM, bipolar membrane; AEM, anion exchange membrane; CEM, cation exchange membrane. Reproduced from ref. 30 with permission from The Royal Society of Chemistry.

CO₂ by electrochemical acidification and simultaneously produces H₂ by electrolysis (33). The cell is composed of three chambers, separated by two cation-exchange membranes, with seawater flowing through the central chamber and with desalinated water in the outer anode and cathode chambers, to avoid the CER and scale deposits. Work is in progress (34) to reduce the series resistance, to limit the amount of desalinated water required, and to further inhibit the scale deposits.

Catalytic Methanol Production

By analogy with photosynthesis (3), one could in principle produce carbon-based fuel directly from water and CO₂:



However, the high thermodynamic stability of the reactant species implies that a large amount of energy is required. Effectively supplying this energy in a single photochemical or electrochemical process remains a fundamental challenge.

Hydrogen and CO₂ can be combined to yield synthetic fuels by the chemical reduction of CO₂ by hydrogenation. Fig. 3A shows, in a modified Latimer–Frost diagram (35), the room temperature Gibbs free energy of creation (CO₂ reduction) and the enthalpy change upon combustion (oxidation) of C₁ chemicals derived from CO₂, as a function of the degree of reduction. Both methanol and methane have high molar oxidation energies, but since methanol is a liquid at room temperature it has a higher volumetric stored energy density.

We see from Fig. 3A that the hydrogenation of CO₂ to form methanol (reaction, Eq. 5a) is (i) slightly exothermic and (ii) entails a net reduction in the number of molecules. In addition, (iii) there is a competing endothermic reaction, the “reverse water–gas shift” (RWGS) reaction (reaction, Eq. 5b), which also consumes H₂ and CO₂:



These three facts have the following implications for methanol synthesis: (i) Heat will be generated from the “chemical energy”

of H₂, which is available for reuse, (ii) the reaction rate increases with increasing reactant pressure (36), and (iii) competition from the RWGS reaction increases with increasing temperature. As shown in the lower part of Fig. 3B and *SI Appendix*, a result of the low exothermicity of the hydrogenation reaction is that the thermodynamic limit for the equilibrium CO₂ conversion at practical temperatures and pressures is below 30% (37).

Furthermore, the thermodynamics of Fig. 3A dictates that the product of the most stable reaction path for CO₂ hydrogenation is methane. Thus, a selective catalyst is required to optimize methanol synthesis. The kinetics of methanol synthesis using a standard Cu/ZnO/Al₂O₃ catalyst (38) is discussed in *SI Appendix* for a simplified “plug flow” reactor geometry. As shown in the upper part of Fig. 3B, whereas a single pass through the reactor cannot surpass the equilibrium conversion, performing multiple separation/recycling loops can produce high conversion at practical temperature and pressure.

A potentially interesting development for our application is the use of microstructured catalytic reactors (39): Reactor channels with transverse dimensions on the millimeter scale have the advantages over larger systems of improved heat control, more efficient catalyst use, and safe operation at high pressure. Other interesting recent progress in the production of methanol by CO₂ hydrogenation are the development of highly selective Ni–Ga catalysts for low-pressure synthesis (40) and the enhancement of the methanol yield by water sorption (41). Finally, the single-step production of higher (C₅₊) liquid hydrocarbon fuels has been demonstrated by a direct CO₂ Fischer–Tropsch hydrogenation process using a CuFeO₂ catalyst (42).

PV Energy Collection

Large-scale crystalline silicon PV technology is undergoing continual development: It is predicted that by the year 2050 commercial PV modules will be available with an efficiency exceeding 20% and a module price of \$0.25/W_{peak} (43). We envisage situating rows of such modules on floating island structures, with optimal inclination and row spacing. For a 20% module efficiency and an average insolation of 220 W/m², a 100-m-diameter island will produce 0.35 MW_{average}. The marine environment, although incurring the disadvantages of increased corrosion and surface fouling, has the advantage over a land-based installation of PV cell cooling by the adjacent seawater. The electrical output of the PV

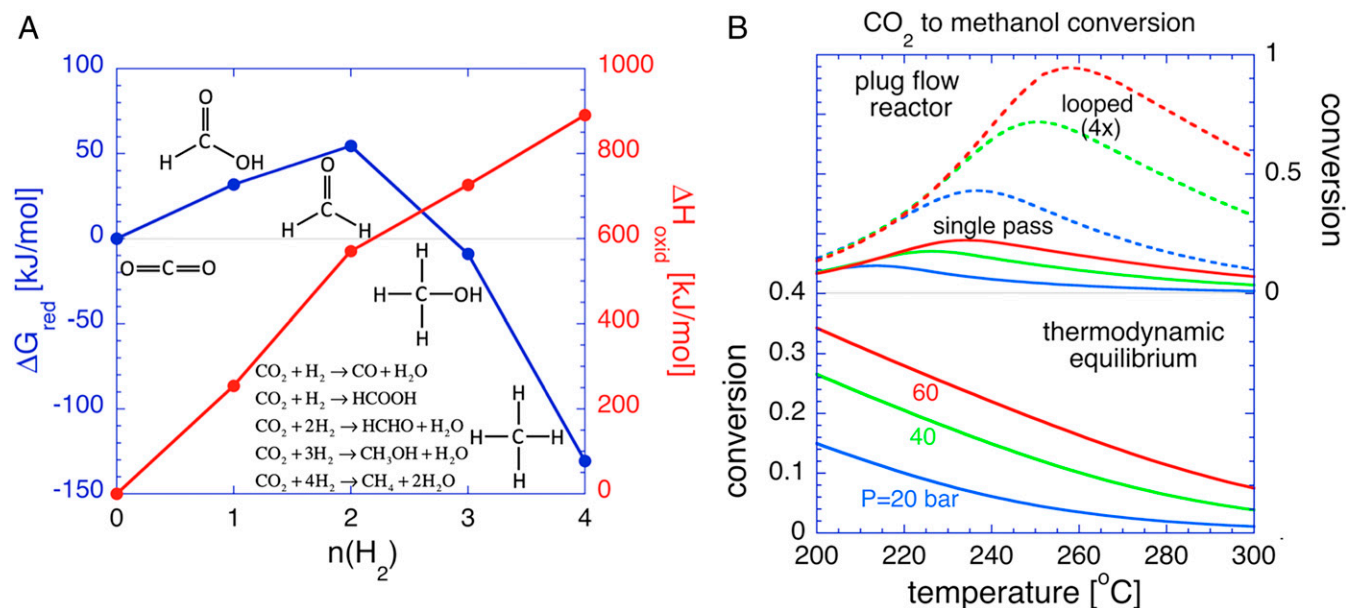


Fig. 3. The production of synthetic fuel. (A) A Latimer–Frost-type diagram showing, at standard temperature and pressure, the change in Gibbs free energy ΔG_{red} upon production by CO_2 reduction by hydrogenation and the change in enthalpy ΔH_{oxid} upon combustion in oxygen, for the C_1 chemicals: formic acid (HCOOH), formaldehyde (HCHO), methanol (CH_3OH), and methane (CH_4). The (slightly) negative value of ΔG_{red} for methanol formation implies an exothermic production reaction, and the large value of ΔH_{oxid} implies a high capacity for chemical energy storage. (B) The thermodynamics (lower part) and kinetics (upper part) of methanol production by the catalytic hydrogenation of CO_2 , according to the reactions of Eq. 5. The lower graph shows the equilibrium molar conversion of CO_2 to MeOH as a function of temperature and pressure (37), and the upper graph shows the predicted molar conversion achieved in a single- and a four-pass plug flow reactor, using a $\text{Cu/ZnO/Al}_2\text{O}_3$ catalyst (38). See *SI Appendix* for details. Note that the conversion in a single-pass reactor cannot exceed the equilibrium value predicted by thermodynamics.

array must be matched to the input of electrolytic cells, at varying levels of solar irradiation, and a particularly elegant method, without the need of active devices, is to optimally configure series/parallel connections of the PV cells with the electrolytic cells (44). It should be noted that an interesting alternative marine-based renewable energy source for distributed H_2 production, CO_2 extraction, and methanol production is off-shore wind turbines (45)—regions with high average winds tend to have low insolation, and vice versa.

Dynamics of Floating Islands

A constraint from a marine technology point of view is that we need low-cost, robust structures for the overall economics of marine solar islands. A plausible structural foundation member for a solar island is a floating elastic torus, similar to the cage support used in aquaculture. A net-like deck, supported by several additional concentric floaters, would carry the PV cells, and the islands would be moored in clusters (Fig. 4A). The equipment for H_2 production, CO_2 extraction, and MeOH catalysis could be mounted on a separate unit, possibly a rigid-hull ship. The island design would profit from the present trends to move floating PV arrays (46) and fish farms (47) to the open ocean: The statistical extreme values of structural stresses and mooring loads based on local and global wind conditions, significant wave height, mean wave period, and wave heading must be considered with regard to operability and survivability. The mechanical stability required for the PV cell mounting needs to be specified, and ship access must be provided for maintenance. Water on deck and slamming loads must be minimized—this can be achieved by using flexible floaters that to a large extent follow the waves. The feasibility of such a structure has been documented in model tests. Autonomous underwater vehicles could perform necessary cleaning of biofouling of the structures.

The preferred materials for the floating tubes and mooring ropes of large-scale floating fish farms are polyethylene and polyamide,

due to their high strength, low weight, low cost, and resistance to attack by UV radiation and chemical agents (48). It should be noted that polyethylene can be efficiently produced from recycled plastic waste (49).

Numerical calculations and model testing have been performed of the dynamics of a single floating elastic torus structure interacting with water waves (50, 51); an approximate linear treatment of torus deflections is presented in *SI Appendix*. Fig. 4B shows the resulting torus deflection amplitude with respect to the water surface, normalized by the incoming wave amplitude, as a function of the wavelength λ of incoming regular waves. Curves are shown for three different values of the island diameter $2R$, and they are superimposed on a typical wave spectrum of a fully developed sea (52). Note that (i) for $\lambda \ll 2R$, the torus is essentially stationary, seeing the full wave amplitude, (ii) for $\lambda \gg 2R$, the torus effectively follows the oscillating water surface, and (iii) resonance effects occur for $\lambda \sim 2R$. Reducing the island diameter shifts the resonant responses out of the wave spectrum. These results have consequences for the optimal island dimensions (*SI Appendix*).

The fact that the deflection amplitudes calculated using the simple linear theory are of the same order as the incoming wave amplitude demonstrates the necessity of quantitative predictions of a more detailed, nonlinear analysis (51). This is particularly true with regard to the inherently nonlinear phenomena of “overtopping” (waves breaking over the upper torus surface) and “out of water” (protrusion of the torus above the water surface).

Solar Island Placement

To investigate possible locations for solar methanol island clusters, we impose the following restrictions: average insolation greater than 175 W/m^2 , 100-y maximum wave height less than 7 m, water depth for island mooring less than 600 m, and a low probability of tropical hurricanes. Compatible regions, shown in Fig. 5A, cover 1.5% of the global ocean surface and together

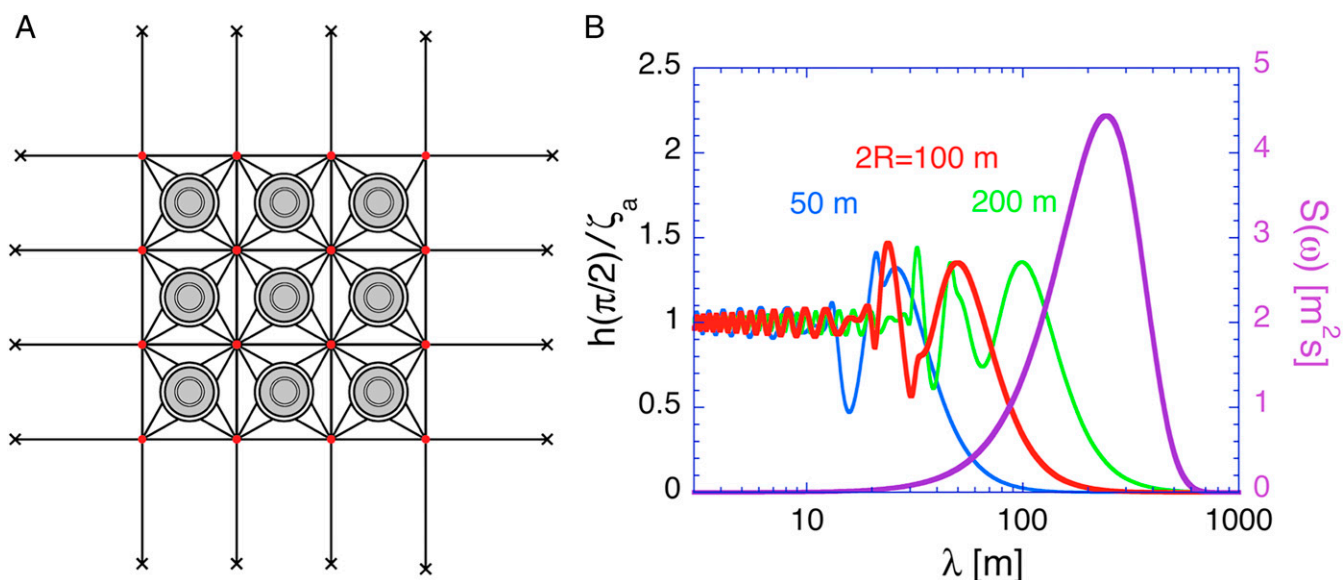


Fig. 4. Marine design considerations for solar methanol islands. (A) A schematic moored arrangement of solar islands carrying PV cells. Each island is based on concentric floating toroidal tubes. (B) Predictions of a simple linear theory (50) for the amplitude h of the vertical motion of a single toroidal tube (evaluated at the angular position $\beta = \pi/2$ around the torus, at right angles to the incoming waves), relative to that of the water surface and normalized by the incoming wave amplitude ζ_a , as a function of the incoming wave wavelength λ , for the three lowest deformation modes: heave, pitch, and fundamental bending. The red curve is for a torus with diameter $2R = 100$ m, minor radius $r = 1.1$ m, and wall thickness $t_w = 0.1$ m, and the blue and green curves are for smaller and larger tori, respectively, with the minor radius scaled to preserve the areal mass density of the island and the condition for 50% draft. The magenta curve shows a typical wave spectrum $S(\omega)$ for a fully aroused sea, for sea state 6 in the North Pacific and North Atlantic, with significant wave height $H_{1/3} = 5$ m and mean wave period $T_1 = 9.6$ s (52). The angular frequency ω and the wavelength λ of the waves are related by the expression for gravity waves. See *SI Appendix* for details.

receive a total average incident radiation of 1.2 PW, implying an average insolation of 220 W/m^2 (see *SI Appendix* for details). Note that suitable locations occur along the coasts of both developed and developing countries. Furthermore, placing solar methanol islands near countries currently exporting oil could offer an alternative business model under the increasingly stringent carbon emission regime of the Paris Agreement. We also note that an argument in favor of many small, dispersed facilities in the open ocean over a few large, shore-based plants is the avoidance of local CO_2 depletion (see *SI Appendix* for details).

Solar Methanol Island Operation

Operational parameters for solar methanol islands, deployed on a large scale, depend on engineering assessments and optimizations. We make the following assumptions: An individual facility is a cluster of 70 flexible PV islands, each 100 m in diameter (total PV area $550,000 \text{ m}^2$), which occupies a total area of $\sim 1 \text{ km}^2$. The islands provide electrical power to a central processing unit, mounted on a rigid ship, which houses the desalination and electrolysis cells for H_2 production, the electrochemical cells for CO_2 extraction, the catalytic reactors and associated machinery for methanol production and separation, batteries for short-term electrical energy storage, a methanol storage tank, and miscellaneous equipment and furnishings. The problems of organic and inorganic membrane fouling by seawater, in particular in the ED cells, are well known in the reverse-osmosis desalination industry and require suitable filtration/pretreatment (53).

With an average insolation of 220 W/m^2 (corresponding to a total incoming solar power of 120 MW) and 20% efficient PV modules, the facility produces an average of $24 \text{ MW}_{\text{el}}$ of electrical power. A physical model for the chemical processing equipment, analyzed using the Aspen Hysys software (54), is proposed in *SI Appendix*: An input seawater flow of 6.2 t/h undergoes reverse osmosis desalination and electrolysis, consuming $18 \text{ MW}_{\text{el}}$ and producing 0.345 t/h H_2 . Some of the produced

oxygen is used to combust excess H_2 to provide process heat. A second, much larger seawater flow, 41,000 t/h, feeds ED cells, which consume $3.7 \text{ MW}_{\text{el}}$, plus $1.4 \text{ MW}_{\text{el}}$ for pumping, and extract the dissolved CO_2 with 59% efficiency, yielding 2.4 t/h CO_2 . This corresponds to 5,700 t/y of carbon. The catalytic reactors and separation units consume $1.3 \text{ MW}_{\text{el}}$, principally for compressors, and produce an output of 1.75 t/h of methanol (and ~ 1 t/h of water). A total of $5.4 \text{ MW}_{\text{th}}$ of thermal energy is released by gas compression and cooling, the exothermic catalytic reaction, and purge gas combustion; $1.8 \text{ MW}_{\text{th}}$ of this energy can be recovered, which is sufficient to drive the reboiler/distillation column for separating methanol from the product water. For detailed analysis of the heat balance see *SI Appendix*. Storage batteries allow operation of the chemical plant to continue during the night. The yearly output of the facility is thus 15,300 t/y of methanol, which is periodically collected by tanker ship.

Potential for CO_2 Emission Avoidance and Effect on Global Climate

The average CO_2 emission, or “energy intensity,” of typical fossil fuels is $\sim 70 \text{ g}(\text{CO}_2)/\text{MJ}$, or 19 gC/MJ , and the corresponding value for methanol is 30.3 gC/MJ . This implies that the conversion by a solar methanol island facility of 5,700 tC/y of carbon would effectively avoid the emission of 3,600 tC/y from fossil fuels. In 2014, the worldwide fossil fuel energy consumption (55) was 130,000 TWh/y, implying the emission of 8.95 GtC/y, and the corresponding numbers for all long-haul ($>160 \text{ km}$) transport (by road, rail, ship, and air) were 8,780 TWh/y and 0.6 GtC/y (56). Thus, $\sim 170,000$ solar methanol island facilities would be needed to compensate the CO_2 emissions from long-haul transport.

From the placement restrictions of Fig. 5A, we can estimate the theoretical maximum emission avoidance of solar methanol island facilities. If 1.5% of the ocean area of $3.62 \times 10^8 \text{ km}^2$ is occupied by facilities, each one $1 \times 1 \text{ km}^2$ in area and placed with an edge-to-edge separation of 300 m, their maximum possible

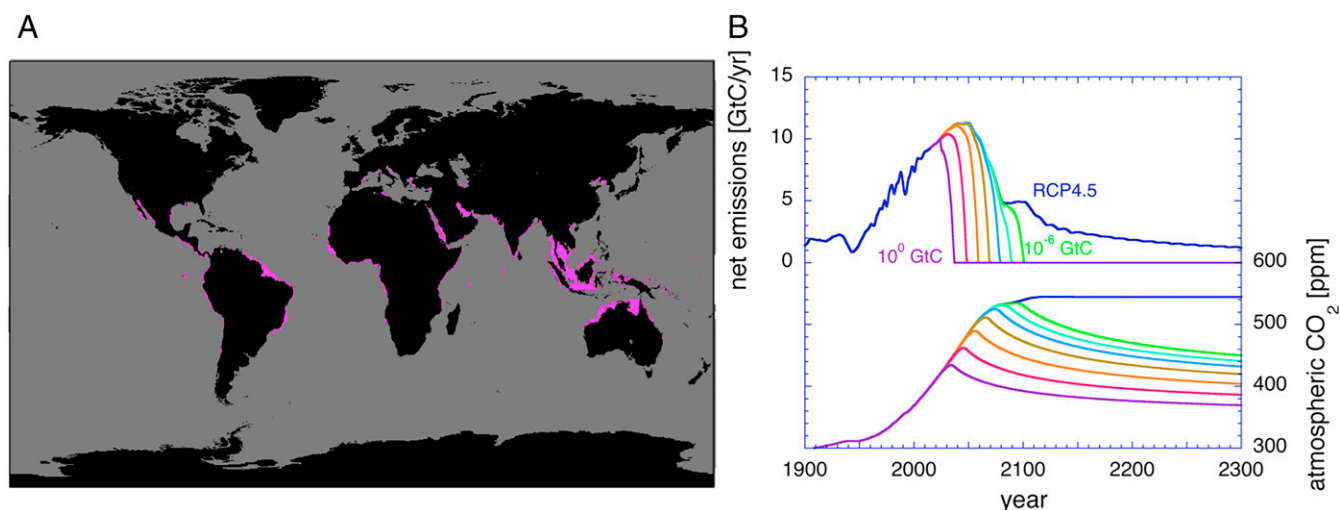


Fig. 5. The geography and climatic influence of solar methanol islands. (A) Geographical locations (magenta) for solar methanol islands satisfying the following physical conditions: average insolation $>175 \text{ W/m}^2$, 100-y maximum wave height $<7 \text{ m}$, water depth $<600 \text{ m}$, and absence of tropical hurricanes (for details see *SI Appendix*). (B, Top) The anthropogenic carbon emissions according to the RCP4.5 (blue curve). The other curves show the net carbon emissions under the assumption that solar methanol island facilities are introduced beginning in the year 2025, with a doubling of capacity every 3.4 y. The various colors correspond to different first-year rates of avoided carbon emission, increasing from 10^{-6} to 10^0 GtC in steps of a factor 10. (B, Bottom) The corresponding evolution of atmospheric CO_2 concentration, based on RCP4.5, without and with solar methanol island clusters. For details of the calculation see *SI Appendix*.

number is 3.2 million. The corresponding avoided emission of 12 GtC/y would then exceed the total global emission from fossil fuels.

What could be the long-term effect on the atmospheric CO_2 concentration of a global introduction of solar methanol island facilities? As a basis, we use the Representative Concentration Pathway RCP4.5, a “medium mitigation scenario” considering CO_2 and other forcing agents used by climate researchers, which presumes a dramatic decline in fossil fuel emissions beginning in 2040 and which leads to a “radiative forcing” (rate of net energy input per unit area to the earth surface and lower atmosphere, measured at the tropopause) in the year 2100 of 4.5 W/m^2 (57).

We make the assumption that beginning in the year 2025 solar methanol island deployment begins with an assumed “first-year” capacity and that the resulting avoided CO_2 emissions thereafter grow exponentially with a doubling time of 3.4 y, equal to that for the current growth of electrical power generation from wind energy (58). For illustration, we vary first-year rates of avoided carbon emission over the range 10^{-6} to 10^0 GtC , in steps of a factor 10. This corresponds to a first-year capacity of less than one facility up to a, rather unrealistic, capacity of 270,000 facilities. We further assume that after the avoided emissions become equal to the RCP4.5 projection, the net emission remains zero—negative emission would require carbon sequestration. In Fig. 5B, Top we show historical and projected anthropogenic carbon emissions for RCP4.5 and the reduction in these emissions that could be realized by solar methanol island development assuming various first-year capacities. In Fig. 5B, Bottom the corresponding projected evolutions of the atmospheric CO_2 concentration are presented. Details of the calculation and projected global temperature evolution are supplied in *SI Appendix*.

Without the introduction of solar methanol islands, model calculations yield a continuous postindustrialization average global temperature rise, which surpasses 3.3°C in 2150. Assuming a first-year (2025) capacity of 270 islands with a first-year emission reduction of 10^{-3} GtC yields zero net carbon emissions in the year 2069 and an approximately stable post-2150 temperature increase of 2.7°C . Note that for a carbon emission avoidance per solar methanol island cluster of 3,600 tC/y, the peak number of facilities required for the 10^{-3} GtC scenario is 2 million and is thus

in the range of the technical potential discussed above. This large figure is a direct consequence of the enormous scale of ongoing and projected fossil carbon emissions. Carbon emission mitigation likely requires a portfolio of measures and technologies to meet the climate targets of the Paris Agreement; our estimate of the technical potential and the results of the illustrative scenarios show that solar methanol islands could be an important element in this portfolio.

Economic Considerations

Methanol has an energy content of 19.7 MJ/kg , so a solar methanol island cluster which consumes 120 MW of incident solar power to produce 15,300 tons/y has an energy storage efficiency of 8.0% and will, during a 20-y lifetime, supply 6,000 TJ of fuel. The cost of energy is closely related to the health of the economy, and it has been argued (59) that the maximum price consistent with economic stability is approximately $\$15/\text{GJ}$, which corresponds to an oil price of $\$92$ per barrel or $\$0.054$ per kWh_{el} . A $\$15/\text{GJ}$ limit implies a maximum allowable cost, including operation, of a solar methanol island facility of $\$90$ million.

The approximate capital costs of major items of a single solar methanol island complex are summarized in *SI Appendix*; published subsystem costs are scaled by capacity using the “0.6 exponent rule” for chemical plants (60). Approximate cost figures are given for the PV modules, the reverse-osmosis desalination equipment, the electrolytic cells for H_2 production, the ED cells for CO_2 extraction, and the catalytic reactor for methanol production. Missing from the summary are the highly uncertain capital costs for seawater pretreatment equipment and the floating island structures. The cost analysis presented in *SI Appendix* is for a single solar methanol island facility; massive worldwide introduction of this technology will bring substantial savings due to economy of scale.

Open Questions

Among the many questions that need to be addressed in more detail for a practical design of solar-powered artificial marine islands to recycle CO_2 into synthetic liquid fuel are the following. How can PV modules be adapted for large-scale deployment in a marine environment, and how can they be efficiently cleaned and

maintained? Can desalination and electrolysis technology be combined to efficiently produce H_2 from seawater? Is ED the optimal method for large-scale CO_2 extraction from seawater, and, if so, what membrane development and systems engineering are required to realize a large, practical marine installation? Is methanol fuel the best choice for the final product, or should one consider producing heavier hydrocarbons on site? What is the optimal design, including reactor looping and heat and pressure management, for a marine-based synthetic fuel reactor and separation system? What is the best practical design for large, floating PV islands with high survivability in marine conditions? How can one optimize their life cycle, and what realistic growth path will have a significant long-term impact on the Earth's climate? Answering these questions will require detailed technological analyses, laboratory and field tests of competing designs, optimization of integrated systems, and refined cost estimates. It

is imperative that innovative solutions are soon realized, to limit the rise in global atmospheric CO_2 concentration.

ACKNOWLEDGMENTS. We thank our colleagues in the Zurich solar methanol group, Davide Bleiner, Chris Rossel, Reto Holzner, Issam Kabbani, Bruno Keller, Karl Knop, and Christine Ledergerber, for stimulating discussions. We also thank Odd Magnus Faltinsen for insights in marine design; Meike Heinz and Ulrich Vogt for discussions of electrochemistry; Heather Willauer for expertise on CO_2 extraction from seawater; James Orr for discussions on marine chemistry; Paul Hsieh for discussions and detailed simulations of local CO_2 depletion; Malte Behrens, Ibrahim Dincer, Payam Esmaili, Nobert Heeb, and Hilde Vennik, for information regarding methanol synthesis; Peng Li, Per Christian Endresen, and Michael Meylan for discussions of floating island stability; Andreas Sterl and Steve Worely for oceanic data; Raphael Semiat for information on large-scale seawater pretreatment and reverse-osmosis desalination; and Eric McFarland and Christophe Ballif for economic considerations of solar energy. F.J. acknowledges support by the Swiss National Science Foundation (Grant 200020_172476). A.B. acknowledges support by the Swiss National Science Foundation (Grant 200021_172662) and the University of Zürich through the University Research Priority Program LightCheC.

- United Nations Climate Change, The Paris Agreement. <https://unfccc.int/process/the-paris-agreement/what-is-the-paris-agreement>. Accessed March 2019.
- M. A. Scibioh, B. Viswanathan, *Carbon Dioxide to Chemicals and Fuels* (Elsevier, Amsterdam, 2018).
- C. Liu, B. C. Colón, M. Ziesack, P. A. Silver, D. G. Nocera, Water splitting-biosynthetic system with CO_2 reduction efficiencies exceeding photosynthesis. *Science* **352**, 1210–1213 (2016).
- A. Goeppert, M. Czaun, J.-P. Jones, G. K. Surya Prakash, G. A. Olah, Recycling of carbon dioxide to methanol and derived products—Closing the loop. *Chem. Soc. Rev.* **43**, 7995–8048 (2014).
- S. Lee, *Methanol Synthesis Technology* (CRC Press, Boca Raton, Florida, 1990).
- M. Kauw, R. M. J. Benders, C. Visser, Green methanol from hydrogen and carbon dioxide using geothermal and/or hydropower in Iceland or excess renewable electricity in Germany. *Energy* **90**, 208–217 (2015).
- B. D. Patterson et al., "Proposed liquid fuel production on artificial islands," in *Conference on Energy, Science and Technology 2015* (Karlsruhe Institute of Technology, Karlsruhe, Germany, 2015), p. 76, Book of Abstracts.
- T. Hinderling, Y. Allani, M. Wannemacher, U. Elsässer, "Solar islands—A novel approach to cost efficient solar power plants" (CSEM Scientific and Tech. Rep. 2007, CSEM, Neuchâtel, Switzerland, 2007), pp. 21–22.
- T. Hinderling, U. Elsässer, M. Wannemacher, Y. Allani, "Man made island with solar energy collection facilities." US Patent 7891351 B2 (2011).
- Novaton, Solar islands. <http://novaton.com>. Accessed March 2019.
- T. Smolinka, E. T. Ojong, J. Garche, "Hydrogen production from renewable energies—Electrolyzer technologies." *Electrochemical Energy Storage for Renewable Sources and Grid Balancing*, P. T. Moseley, Ed. (Elsevier, Amsterdam, 2015).
- A. T. Marshall, S. Sunde, M. Tsyppin, R. Tunold, Performance of a PEM water electrolysis cell using $Ir_xRu_{1-x}O_2$ electrocatalysts for the oxygen evolution electrode. *Int. J. Hydrogen Energy* **32**, 2320–2324 (2007).
- F. Gutmann, O. J. Murphy, "The electrochemical splitting of water." *Modern Aspects of Electrochemistry*, J. O. M. Ockris, B. E. Conway, Eds. (Plenum Press, New York, 2010), vol. 15, pp. 1–82.
- J. E. Bennett, Electrodes for generation of hydrogen and oxygen from seawater. *Int. J. Hydrogen Energy* **5**, 401–408 (1980).
- J. Rossmel, Z.-W. Qu, H. Zhu, G.-J. Kroes, J. K. Nørskov, Electrolysis of water on oxide surfaces. *J. Electroanal. Chem.* **607**, 83–89 (2007).
- H. A. Hansen et al., Electrochemical chlorine evolution at rutile oxide (110) surfaces. *Phys. Chem. Chem. Phys.* **12**, 283–290 (2010).
- Z. Kato et al., The influence of coating solution and calcination condition on the durability of $Ir_{1-x}Sn_xO_2/Ti$ anodes for oxygen evolution. *Appl. Surf. Sci.* **388**, 640–644 (2016).
- R. W. Stoughton, M. H. Lietzke, Calculation of some thermodynamic properties of sea salt solutions at elevated temperatures from data on NaCl solutions. *J. Chem. Eng. Data* **10**, 254–260 (1965).
- B. Sauvet-Golichon, Ashkelon desalination plant—A successful challenge. *Desalination* **203**, 75–81 (2007).
- R. Semiat, Energy issues in desalination processes. *Environ. Sci. Technol.* **42**, 8193–8201 (2008).
- N. T. Carter, "Desalination and membrane technologies" (Congressional Research Service Rep. 7-5700, Congressional Research Service, Washington, DC, 2015).
- I. Zaslavski, H. Shemer, D. Hasson, R. Semiat, Electrochemical $CaCO_3$ scale removal with a bipolar membrane system. *J. Membr. Sci.* **445**, 88–95 (2013).
- E. Baniasadi, I. Dincer, G. F. Naterer, Electrochemical analysis of seawater electrolysis with molybdenum-oxo catalysts. *Int. J. Hydrogen Energy* **38**, 2589–2595 (2013).
- R. Socolow et al., "Direct air capture of CO_2 with chemicals: A technology assessment for the APS panel on public affairs" (American Physical Society, College Park, MD, 2011).
- C. Gebald, J. A. Wurzbacher, P. Tingaut, T. Zimmermann, A. Steinfeld, Amine-based nanofibrillated cellulose as adsorbent for CO_2 capture from air. *Environ. Sci. Technol.* **45**, 9101–9108 (2011).
- R. E. Zeebe, D. Wolf-Gladrow, *CO_2 in Seawater: Equilibrium, Kinetics, Isotopes* (Elsevier Oceanography Series, Elsevier, New York, 2001), vol. 65.
- W. Wang, R. Nemani, Dynamics of global atmospheric CO_2 concentration from 1850 to 2010. *Biogeosciences Discuss.* **11**, 13957–13983 (2014).
- R. E. Zeebe, D. A. Wolf-Gladrow, H. Jansen, On the time required to establish chemical and isotopic equilibrium in the carbon dioxide system in seawater. *Mar. Chem.* **65**, 135–153 (1999).
- A. E. Al-Rawafteh, H. Glade, H. M. Qiblawey, J. Ulrich, Simulation of CO_2 release in multiple-effect distillers. *Desalination* **166**, 41–52 (2004).
- M. D. Eisman et al., CO_2 extraction from seawater using bipolar membrane electrodialysis. *Energy Environ. Sci.* **5**, 7346–7352 (2012).
- E. Drioli, E. Curcio, G. Di Profio, State of the art and recent progresses in membrane contactors. *Chem. Eng. Res. Des.* **83**, 223–233 (2005).
- M. D. Eisman et al., Indirect ocean capture of atmospheric CO_2 : Part II. Understanding the cost of negative emissions. *Int. J. Greenhouse Gas Control* **70**, 254–261 (2018).
- H. D. Willauer, F. DiMascio, D. R. Hardy, F. W. Williams, Feasibility of CO_2 extraction from seawater and simultaneous hydrogen gas generation using a novel and robust electrolytic cation exchange module based on continuous electrodeionization technology. *Ind. Eng. Chem. Res.* **53**, 12192–12200 (2014).
- H. D. Willauer, F. DiMascio, D. R. Hardy, F. W. Williams, Development of an electrolytic cation exchange module for the simultaneous extraction of carbon dioxide and hydrogen gas from natural seawater. *Energy Fuels* **31**, 1723–1730 (2017).
- W. H. Koppenol, J. D. Rush, Reduction potential of the CO_2/CO_2^- couple. A comparison with other C_1 radicals. *J. Phys. Chem.* **91**, 4429–4430 (1987).
- A. Bansode, A. Urakawa, Towards full one-pass conversion of carbon dioxide to methanol and methanol-derived products. *J. Catal.* **309**, 66–70 (2014).
- J. Skrzypek, M. Lachowska, D. Serafin, Methanol synthesis from CO_2 and H_2 : Dependence of equilibrium conversions and exit equilibrium concentrations of components on the main process variables. *Chem. Eng. Sci.* **45**, 89–96 (1990).
- G. H. Graaf, H. Scholtens, E. J. Stamhuis, A. A. C. M. Beenackers, Intra-particle diffusion limitations in low-pressure methanol synthesis. *Chem. Eng. Sci.* **45**, 773–783 (1990).
- A. Renken, L. Kiwi-Minsker, Microstructured catalytic reactors. *Adv. Catal.* **53**, 47–122 (2010).
- F. Studt et al., Discovery of a Ni-Ga catalyst for carbon dioxide reduction to methanol. *Nat. Chem.* **6**, 320–324 (2014).
- A. Zachopoulos, E. Heracleous, Overcoming the equilibrium barriers of CO_2 hydrogenation to methanol via water sorption: A thermodynamic analysis. *J. CO₂ Util.* **21**, 360–367 (2017).
- Y. H. Choi et al., Carbon dioxide Fischer-Tropsch synthesis: A new path to carbon-neutral fuels. *Appl. Catal. B* **202**, 605–610 (2017).
- V. Sivaram, S. Kann, Solar power needs a more ambitious cost target. *Nat. Energy* **1**, 16036 (2016).
- O. Atlam, F. Barbir, D. Bezmalinovic, A method for optimal sizing of an electrolyzer directly connected to a PV module. *Int. J. Hydrogen Energy* **36**, 7012–7018 (2011).
- Global Wind Energy Council, "Global Wind 2017 report—A snapshot of top wind markets in 2017: Offshore wind, Global Wind Energy Council" (Global Wind Energy Council, Brussels).
- M. Rosa-Clot, G. M. Tina, *Submerged and Floating Photovoltaic Systems* (Academic Press, 2017).
- J. Ryan, "Farming the deep blue." G. Mills, D. Maguire, Eds. (Bord Iascaigh Mhara—Irish Sea Fisheries Board (BIM) & Irish Marine Institute, Dublin, 2004).
- S. D. Weller, L. Johanning, P. Davies, S. J. Banfield, Synthetic mooring ropes for marine renewable energy applications. *Renew. Energy* **83**, 1268–1278 (2015).
- L. Nguyen, G. Y. Hsuan, S. Spataro, Life cycle economic and environmental implications of pristine high density polyethylene and alternative materials in drainage pipe applications. *J. Polym. Environ.* **25**, 925–947 (2017).
- P. Li, "A theoretical and experimental study of wave-induced hydroelastic response of a circular floating collar," PhD thesis, NTNU, Trondheim (2017).
- P. Li, O. M. Faltinsen, C. Lugni, Nonlinear vertical accelerations of a floating torus in regular waves. *J. Fluids Structures* **66**, 589–608 (2016).
- O. M. Faltinsen, *Sea Loads on Ships and Offshore Structures* (Cambridge Ocean Technology Series, Cambridge University Press, 1990).

53. N. Voutchkov, Considerations for selection of seawater filtration pretreatment system. *Desalination* **261**, 354–364 (2010).
54. M. Hillestad M et al., Improving carbon efficiency and profitability of the biomass to liquid process with hydrogen from renewable power. *Fuel* **234**, 1431–1451 (2018).
55. H. Ritchie, M. Roser, Fossil fuels. *Ourworldindata*. <https://ourworldindata.org/fossil-fuels>. Accessed March 2019.
56. D. J. Davis et al., Net-zero emissions energy systems. *Science* **360**, eaas9793 (2018).
57. D. P. van Vuuren et al., The representative concentration pathways: An overview. *Clim. Change* **109**, 5–31 (2011).
58. REN21, “Renewables 2014–Global status report” (REN21, Paris, 2014).
59. E. W. McFarland, Solar energy: Setting the economic bar from the top-down. *Energy Environ. Sci.* **7**, 846–854 (2014).
60. R. Williams, Six-tenths factor aids in approximating costs. *Chem. Eng.* **54**, 124–125 (1947).